Original Research

Magnetic Resonance Detection of Kidney Iron Deposition in Sickle Cell Disease: A Marker of Chronic Hemolysis

Aaron Schein, MD,[1,2] Cathleen Enriquez, BS,[4] Thomas D. Coates, MD,[3] and John C. Wood, MD, PhD[2,4]*

Purpose: To study the pattern, etiology, and significance of renal iron accumulation in chronically transfused sickle cell disease (SCD) and thalassemia major (TM) patients using magnetic resonance imaging (MRI).

Materials and Methods: Magnetic resonance imaging (MRI) was performed in 75 SCD patients, 73 TM patients, and 16 healthy controls. Multiecho gradient echo protocols were used to measure T2* reciprocals (R2*) in the kidney, liver, and heart. Kidney R2* was compared to tissue iron estimates, serum iron markers, and surrogates of intravascular hemolysis by univariate regression.

Results: Mean R2* in SCD patients was 55.3 ± 45.3 Hz, compared with 22.1 ± 11 Hz in TM patients and 21.3 ± 5.8 Hz in control subjects ($P < 0.001$). Kidney R2* decreased with advancing age ($R^2 = 0.09$, $P < 0.02$). Kidney R2* correlated strongly with increased serum lactate dehydrogenase levels found in SCD ($R^2 = 0.55$, $P < 0.001$), but was independent of hepatic iron concentration and cardiac R2*. Kidney R2* did not correlate with blood pressure, creatinine, cardiac index, or right and left ejection fraction.

Conclusion: Intravascular hemolysis, not chronic transfusion, causes renal hemosiderosis in SCD. Prospective trials are necessary to determine whether kidney R2* is a biomarker for hemolysis-mediated vascular complications in SCD.

Key Words: kidney; iron; relaxometry; sickle cell disease; hemolysis; thalassemia
J. Magn. Reson. Imaging 2008;28:698–704.

DISORDERS OF HEMOGLOBIN SYNTHESIS such as sickle cell disease (SCD) and thalassemia major (TM) represent the most common genetic diseases worldwide, striking over 270 million people (1). In nations with sufficient resources, severely affected patients are treated by blood transfusions every 3–4 weeks. Unfortunately, this therapy produces iron overload in various tissues including the liver, heart, and endocrine tissues, leading to life-threatening complications (2). Iron chelation therapy can ameliorate these complications but close monitoring of tissue iron is important to track iron accumulation and iron removal therapies. Serial biopsy is impractical because of significant patient discomfort, procedural risk, and wide sampling variation (3). Furthermore, many of the "target" organs are not amenable to biopsy. Recently, magnetic resonance imaging (MRI) gradient echo (T2*) and spin echo (T2) techniques have been developed to quantify tissue iron stores in the liver and the heart (4,5). The reciprocal of T2*, known as R2*, has been shown to rise linearly with chemically determined tissue iron concentration in both liver and heart (4,6,7).

The kidney is another site of iron accumulation in SCD and thalassemia (8–10). Unlike in the other organs, it is unclear whether kidney iron results solely from intravascular hemolysis, chronic transfusion therapy, or both (10–13). Further, while iron accumulation in the heart and liver is well known to lead to life-threatening complications such as cardiomyopathy and cirrhosis, the significance of iron in the kidney is poorly understood (2,8–10,14–20).

Our aim in this study was to use kidney R2* as a surrogate for kidney iron to retrospectively examine the pattern, etiology, and significance of renal iron accumulation in chronically transfused patients with SCD and thalassemia. In particular, we sought to answer the following questions. 1) What is the prevalence and distribution of iron in the kidney in these two disorders? 2)

[1]Department of Diagnostic Radiology, Keck School of Medicine, University of Southern California, Los Angeles, California.
[2]Department of Pediatric Radiology, Children's Hospital, Los Angeles, California.
[3]Division of Pediatric Hematology, Children's Hospital, Los Angeles, California.
[4]Division of Pediatric Cardiology, Children's Hospital, Los Angeles, California.

Contract grant sponsor: National Heart, Lung, and Blood Institute (NHLBI); Contract grant number: 1 RO1 HL075592-01A1; Contract grant sponsor: General Clinical Research Center at Childrens Hospital Los Angeles; Contract grant number: RR000043-43; Contract grant sponsor: Center for Disease Control (Thalassemia Center Grant); Contract grant number: U27/CCU922106; Contract grant sponsor: Novartis Pharma.

*Address reprint requests to: Dr. John C. Wood, MD, PhD, Department of Radiology, Mail Stop 81, Children's Hospital of Los Angeles, 4650 Sunset Blvd., Los Angeles, CA, 90027. E-mail: jwood@chla.usc.edu

Received January 14, 2008; Accepted June 4, 2008.
DOI 10.1002/jmri.21490
Published online in Wiley InterScience (www.interscience.wiley.com).

Does iron accumulation in the kidney better correlate with transfusion burden or hemolysis? 3) Are there links between kidney R2* signal and signs of renal or nonrenal disease?

MATERIALS AND METHODS

Patient Population

Patient selection and informatics methods were approved by the Institutional Review Board (IRB). Due to the retrospective nature of this study a waiver was obtained from the IRB and informed consent was not required of patients. Clinical information was obtained from all SCD and thalassemia patients for whom clinically indicated MRI examinations were performed at Children's Hospital, Los Angeles between Jan 1, 2000 and July 1, 2007. All MRI and laboratory studies were performed as standard of care and were retrieved from the patient's electronic record. Lab values were restricted to within 1 year of the MRI examination date. All patients included in this analysis received chronic transfusion therapy consisting of 10–15 cc/kg transfusions performed every 3–4 weeks to maintain a pretransfusion hemoglobin of 9–10 g/dL. Indications for chronic transfusion in the SCD population included prior stroke, abnormal transcranial Doppler examination, recurrent acute chest, and intractable pain crises. Hemoglobin S concentration was maintained below 30% per stroke prophylaxis guidelines. All patient information was communicated in a manner compliant with the Health Insurance Portability and Accountability Act (HIPAA).

Normal Reference Values

Sixteen healthy volunteers were recruited to provide normal kidney R2* reference values; all subjects gave informed consent. All volunteers were selected based on their absence of current or historical hemolytic anemia, blood transfusion, or kidney disease. Kidney R2* in the volunteers was measured in the same manner as the patients. There were seven men and nine women with a mean age of 24.9 ± 1.3 (mean ± SD) years.

MRI Measurements

Cardiac and liver MRI measurements were performed as previously described by Wood et al and Ghugre et al (7,21). Briefly, we used a four-element torso coil on a 1.5T General Electric CVi scanner (GE Medical Systems, Milwaukee, WI). Liver R2 was measured in four axial slices using a 90°–90° spin echo sequence with echo times of 3, 3.5, 5, 9, 18, and 30 msec, collecting a single echo time (TE) per 16-second breath-hold. Liver R2* was estimated using a multiphase single-echo gradient echo technique with echo times spaced logarithmically from 0.95–16 ms. Other imaging parameters included a 48 × 24 cm field of view (FOV), 64 × 64 matrix, 10 mm slice thickness, 25 msec repetition time (TR), 20° flip angle, and 83 kHz bandwidth. This gradient echo technique is optimized for the high R2* (>1000 Hz) observed in heavily iron loaded patients. Kidney R2* was measured in five coronal slices using a multiecho-gradient echo R2* method with echo times equally spaced from 1.2–13.9 msec. Other imaging parameters include 40 × 30 cm FOV (extra phases acquired to prevent phase wrap), 128 × 128 matrix, 5 mm slice thickness, 100 msec TR, 20° flip angle, and 83 kHz bandwidth.

Signal decay across increasing echo times was fit to a constant-plus-monoexponential model for each pixel in the image, forming relaxivity maps of the heart, liver, and kidney, as described by Wood et al (4,21). Regions of interest (ROIs) were drawn about the entire liver and kidney and the mean R2* value was calculated from the R2* map; ROI in the heart was restricted to the interventricular septum, as described by Wood and colleagues (21).

Hepatic iron concentration (HIC) could be directly estimated in the liver using previously validated calibration curves (4). No similar curves exist for heart and kidney; thus, the mean R2* was used as a surrogate for relative iron concentration in these tissues. Cardiac R2* was used as a surrogate for nontransferrin-bound iron, and liver R2* as a surrogate for total body iron balance.

Because SCD is associated with hyperfiltration, kidney volumes were estimated from MR images by an ellipsoid method (22). Kidney volumes were normalized to patient body surface area.

Statistical Analysis

A nonpaired Student's *t*-test was used to detect differences in continuous variables between two populations. Standard univariate least-squares linear regression was used to measure the Pearson's correlation coefficient between continuous variables in most cases. A bivariate analysis model was used to examine the relationship between age, serum creatinine, and kidney R2* in SCD patients. A $P \leq 0.05$ level was considered statistically significant.

RESULTS

We studied 148 patients, including 73 with thalassemia and 75 with SCD. Table 1 demonstrates their demographics. Key differences between the two patient populations are as follows. Thalassemia patients were older and had lower liver iron, ferritin, systolic blood pressure, and cardiac index. Despite having lower iron stores, patients with thalassemia trended toward higher transferrin saturation (78.2 ± 20.2 vs. 67.4 ± 24.9, $P < 0.06$). SCD patients had greater markers of hemolysis, including reticulocyte count (9.61% vs. 1.83%, $P < 0.001$) and serum lactate dehydrogenase (LDH; 1327 U/L vs. 444 U/L, $P < 0.001$). Kidney volumes, body surface area (BSA), heart rate (HR), diastolic blood pressure, mean blood pressure, and hemoglobin did not differ between the two groups.

In addition, sickle cell and thalassemia patients had obvious differences in kidney appearance on gradient echo imaging. Figure 1 demonstrates coronal gradient echo images at the first four echo times for two representative patients. The TM patient (top panel) demonstrates little kidney darkening or tissue contrast with

Table 1
Patient Demographics

	Sickle Cell Disease	Thalassemia	P^a
n	75	73	—
Males, *n* (%*n*)	34 (45.3)	41 (56.2)	
Females, *n* (%*n*)	41 (54.7)	32 (43.8)	0.019[b]
Age (years), mean ± SD	14.6 ± 6.4	19.3 ± 10.5	0.002[c]
Body surface area (m^2)	1.34 ± 0.39 (70)	1.35 ± 0.37 (72)	0.824
Left kidney volume/BSA (mL/m^2)	91.9 ± 25.8 (53)	87.9 ± 30.9 (67)	0.444
Right kidney volume/BSA (mL/m^2)	90.0 ± 20.7 (53)	86.9 ± 18.3 (67)	0.399
Mean kidney volume/BSA (mL/m^2)	90.9 ± 21.6 (53)	87.4 ± 21.7 (67)	0.378
Hepatic iron concentration (mg/g dry)	15.0 ± 11.2 (73)	11.2 ± 10.3 (72)	0.004[c]
Systolic blood pressure (mm Hg)	108 ± 10 (75)	105 ± 12 (73)	0.032[c]
Diastolic blood pressure (mm Hg)	62 ± 12 (75)	60 ± 11 (73)	0.337
Mean arterial pressure (mm Hg)	78 ± 10 (75)	75 ± 10 (73)	0.126
Heart rate (beats/min)	80 ± 17 (74)	77 ± 17 (71)	0.099
Cardiac index ($L/min*m^2$)	4.61 ± 0.93 (29)	4.09 ± 0.89 (38)	0.025[c]
Hemoglobin (g/dL)	9.9 ± 1.4 (35)	10.2 ± 1.7 (40)	0.367
Ferritin (ng/mL)	4015 ± 4325 (38)	2337 ± 2130 (57)	0.034[c]
Transferrin saturation (%)	67.4 ± 24.9 (28)	78.2 ± 20.2 (47)	0.056
Reticulocyte (%)	9.61 ± 7.84 (33)	1.83 ± 1.63 (24)	<0.001[c]
Lactate dehydrogenase (U/L)	1327 ± 786 (31)	444 ± 245 (39)	<0.001[c]

BSA, body surface area.
The above values represent mean ± SD (*n*), unless otherwise specified.
[a]Calculated using Student's *t*-test, unless otherwise specified.
[b]Calculated using Fisher's exact test.
[c]Represents a statistically significant value ($P < 0.05$).

increasing echo time. Mean R2* over both kidneys was 17 Hz. In contrast, the SCD patient (bottom panel) exhibits striking cortical darkening with relative sparing of the renal medulla and pelvis. Mean R2* over both kidneys was 180 Hz, although darkest areas had much greater R2* values. Not surprisingly, the liver darkens rapidly in both patients; splenic iron is also prominent in the SCD patient.

Figure 2 highlights the disparity between the two patient groups and the group of normal subjects. Control subjects had a kidney R2* of 21.3 Hz ± 5.8 (13–32 Hz) with a 95% confidence limit of 33.7 Hz. Kidney R2*

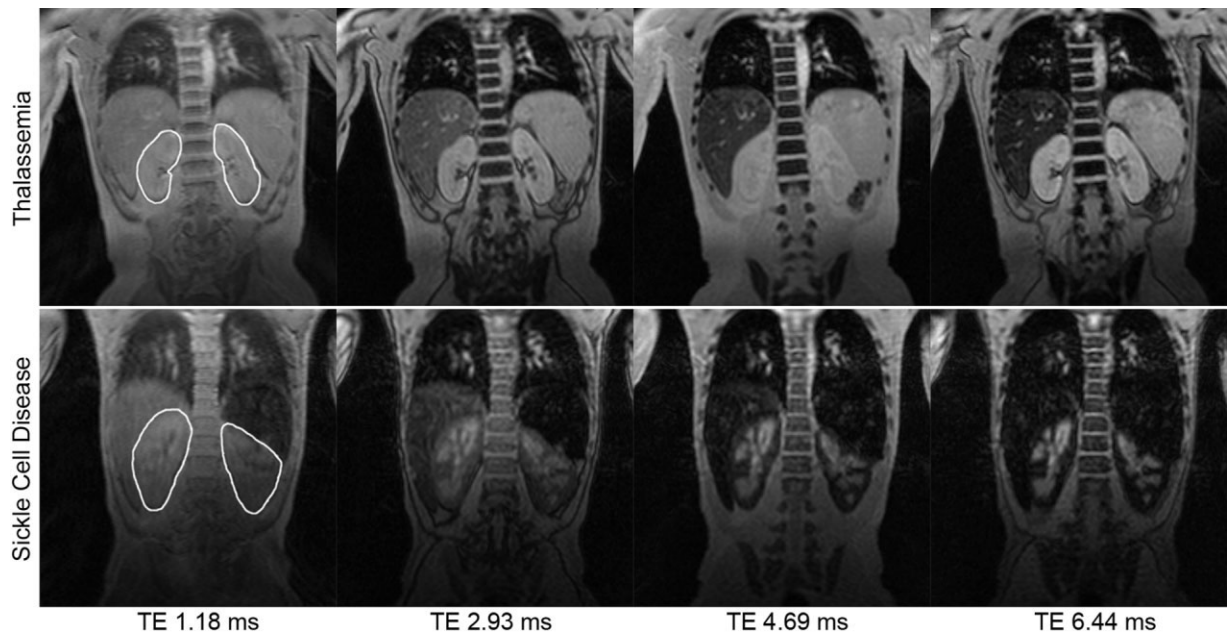

Figure 1. Comparison of kidney T2*-weighted images in sickle cell disease and thalassemia. Representative T2*-weighted coronal MR images of the kidneys at the first four echo times (TE) from a 10-year-old with thalassemia (top) and a 14-year-old with sickle cell disease (bottom). The region of interest for analysis is shown in the leftmost images. The thalassemia and sickle cell disease patients had mean kidney R2* values of 17 Hz and 180 Hz, respectively. Note also the T2* signal attenuation in the livers of both patients and in the spleen of the SCD patient.

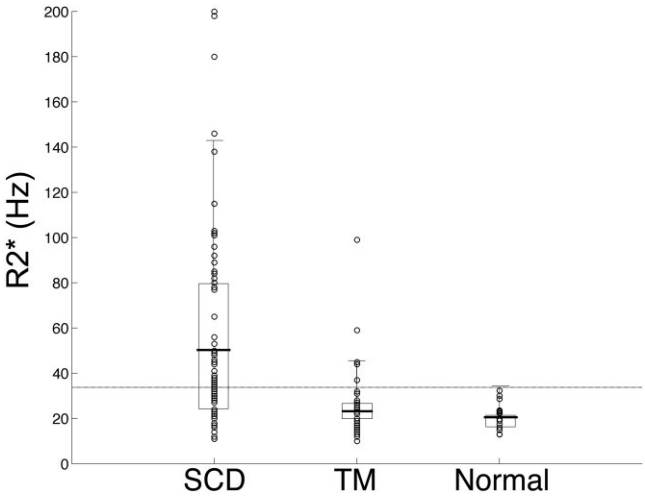

Figure 2. Comparison of kidney R2* in sickle cell disease and thalassemia. Boxplot analysis demonstrates mean kidney R2* (thick horizontal bars) of 55.3 ± 45.3 Hz for SCD patients (n = 75), 21.9 ± 12.2 Hz for thalassemia (n = 73) patients, and 22.0 ± 6.2 Hz for normal volunteers (n = 16). Rectangles indicate 25th to 75th percentiles and error bars represent 2 SD. The horizontal gray line represents the 95% confidence interval for normal reference values (33.7 Hz). Mean R2* in SCD patients was statistically different from both TM patients and normal volunteers ($P < 0.001$).

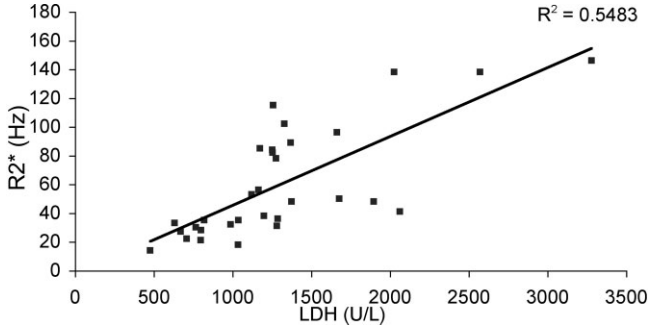

Figure 4. Kidney R2* as a function of lactate dehydrogenase (LDH) in sickle cell disease. Kidney R2* was strongly correlated with LDH in SCD patients (n = 31, $P < 0.001$).

from TM patients had a similar distribution, 21.9 ± 12.2 Hz (10–99 Hz), with 5/73 (6.8%) patients outside the normal range. SCD patients had a mean kidney R2* of 55.3 ± 45.3 Hz (11–200 Hz), with 39/75 (52%) patients outside of the normal range; these values were statistically significant with respect to both control subjects and TM patients ($P < 0.001$). There were no systemic R2* differences between left and right kidneys; the coefficient of variation was 13% in the SCD patients and 44% in the TM patients. Within each kidney, slice-to-slice variability had a coefficient of variation of 18.9%; this was reduced to 7.7% by averaging six slices together.

Standard least-squares regression analysis revealed no correlation between kidney R2* and hepatic iron concentration (P = 0.87), which is the single best marker of total body iron burden (23,24). Kidney R2* also did not correlate with heart R2* (data not shown). Kidney R2* fell with increasing age (R^2 = 0.09, $P < 0.02$, Fig. 3, left panel), whereas HIC rose with increasing age (R^2 = 0.08, $P < 0.02$, Fig. 3, right panel), further reinforcing the independence of kidney R2* and liver iron.

While kidney R2* failed to correlate with iron deposition in other tissues, it was positively correlated with LDH levels (R^2 = 0.55, $P < 0.001$, Fig. 4) in SCD patients. Of note, all of the patients with detectable kidney iron had LDH values greater than 1000, more than 7 SD above the mean (normal range 466 ± 76); none of the thalassemia patients had LDH values greater than 1000. Serum LDH is a clinically acceptable surrogate for hemolysis in SCD because the contribution from red blood cells swamps those from other cell types (25). LDH was negatively correlated with serum arginine (r^2 = 0.43), arginine/ornithine (r^2 = 0.25), and arginine/(ornithine + citrulline) ratios (r^2 = 0.32), reflecting arginase release from hemolyzed red cells and further strengthening the relation between serum LDH and hemolysis (data not shown) (26).

However, kidney R2* did not correlate with any other biomarkers of SCD severity, including systolic blood pressure (SBP); diastolic blood pressure (DBP); cardiac E/A ratio; reticulocyte count; hematocrit; hemoglobin; left or right ventricular ejection fraction (LVEF and RVEF, respectively); right, left, or mean kidney volume, standardized to BSA; serum aspartate aminotransferase (AST); or alanine aminotransferase (ALT). Interestingly, serum creatinine concentration (Cr) correlated *negatively* with kidney R2* (R^2 = 0.171, P = 0.018). This association was confounded by age, however, and

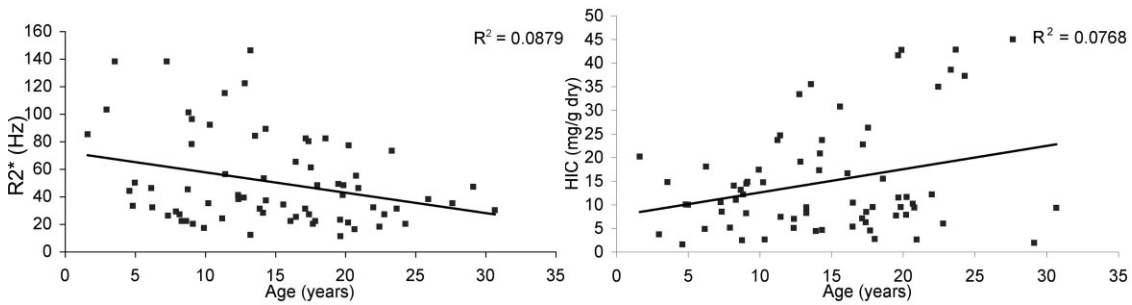

Figure 3. Effect of age on kidney R2* and HIC in SCD patients. Kidney R2* declined weakly with age (left panel, P = 0.013). In contrast, HIC tended to rise with age (right panel, P = 0.018), reinforcing the independence between these variables.

multivariate regression weakened the kidney R2* association to borderline significance ($P = 0.10$).

DISCUSSION

The goal of this study was to describe the pattern of iron distribution in the kidney in SCD and thalassemia, gain insight into its mechanism, and investigate its functional significance. We found kidney iron only in the cortices of SCD patients, a pattern that is consistent with anatomic and prior imaging studies (9). The cortices contain the highest concentrations of glomeruli and proximal tubules—the microanatomic locations containing the greatest iron deposition in SCD patients (8). Although MRI has insufficient resolution to distinguish between glomerular and tubular iron, the iron deposits likely localize to the tubular system as proximal tubules contain avid heme transport molecules. Specifically, megalin, a 600-kD low-density lipoprotein family transmembrane glycoprotein, and cubulin, a 460-kD glycoprotein that assists megalin, bind to and internalize free circulating hemoglobin (12). Circulating free hemoglobin is generally maintained at low levels through scavenging by circulating haptoglobin, preventing heme filtration. Haptoglobin-hemoglobin complexes are efficiently removed by the liver and reticuloendothelial system; however, this buffering system may be overwhelmed in the face of chronic or massive hemolysis. It is notable that all of the patients with detectable kidney iron had LDH values over 1000.

Our results cannot definitively exclude the possibility that gross kidney iron accumulation results from intrarenal red cell sickling, microinfarction, and hemorrhage rather than intravascular hemolysis per se (8,15,20,27). Since the severity of SCD and the severity of hemolysis are tightly coupled, it might be impossible to distinguish between these mechanisms. However, we did not see high iron deposition in the renal pyramids where microvascular occlusion is worst. Furthermore, MRI-detectable renal iron has been qualitatively described in nonsickle hemolytic diseases (including paroxysmal nocturnal hemoglobinuria and mechanical heart valves), suggesting that hemolysis is causative rather than simply correlative (28–34); we have also documented heavy renal cortical siderosis in patients with pyruvate kinase and congenital dyserythropoetic anemia (not shown). Thus, the pattern of iron deposition, the strong correlation of kidney iron with LDH but not liver iron, the prevalence of cortical kidney iron in other hemolytic anemias, and the near absence of MRI-detectable kidney iron in the thalassemia population suggest that elevated circulating free hemoglobin from chronic hemolysis is the dominant causative agent for kidney iron deposition in transfused SCD patients.

If hemolysis causes kidney iron deposition, why didn't kidney iron increase steadily with age? For nontransfused SCD patients, we postulate that it would. However, all of the patients in this study received chronic transfusions to suppress endogenous sickle hemoglobin production, reduce SCD complications, and enable more normal growth. Data from the STOP study (35) demonstrate a 60% reduction in circulating free hemoglobin when transfusions were initiated. Patient age in our series indirectly reflects years of transfusion therapy (as suggested by the upward trend of liver iron with age), and so older patients will generally have experienced lower average hemolytic rates during their lifetimes. Thus, chronic reduction of circulating free hemoglobin, along with somatic growth and chelation therapy, appears to decrease kidney iron concentration over time.

The near absence of detectable renal iron in TM patients was somewhat surprising. Thalassemia patients do experience hemolysis; however, their anemia is characterized more by ineffective erythropoeisis (36). Reticulocyte counts and LDH levels were normal in our thalassemia patients, in marked contrast to those with SCD. But despite our failure to find radiographically detectable iron, a number of investigators have claimed that iron damages thalassemic kidneys (16–19,37,38). In particular, proximal tubular dysfunction (common in children and adults with thalassemia major) correlates with transfusional iron burden (17,37). While we cannot exclude that iron plays a role in the pathophysiology of this tubular dysfunction, our data suggests that renal iron toxicity in thalassemia would have to occur at concentrations below the MRI detection limit.

The pathophysiologic significance of kidney R2* is unclear. It may have value as a long-term measure of hemolysis in those with hemolytic disease, much in the same way as glycosylated hemoglobin (HbA1C) serves as a long-term measure of serum glucose among diabetics. Chronic hemolysis depletes serum arginine (as observed in our population), lowering nitric-oxide bioavailability and decoupling nitric-oxide synthetase. These changes, in turn, produce systemic and pulmonary vascular disease, increased vascular adhesion, increased airway reactivity, and restrictive lung disease (25,26). Pulmonary hypertension (PHT) is the cause of death in more than 25% of SCD-related mortalities (39). Measures of arginine bioavailability, cell free hemoglobin, and LDH have all been shown to predict both the incidence of PHT and mortality in SCD patients (26). Since these serum markers are relatively labile, it is an open question whether kidney R2* might provide a more robust prognostic tool for subsequent vascular disease. In the present study our patients on chronic transfusion were young, generally free from overt pulmonary or systemic vascular disease, and many did not have current echocardiograms, making it difficult to establish any correlation between kidney R2*, pulmonary hypertension, and diastolic dysfunction.

Beyond its value as a putative indicator of hemolysis, the role of iron deposition in the kidney in SCD nephropathy is largely unknown. Renal failure is common in SCD, occurring in nearly 30% of all SCD patients at the time of their death (40). Kidney damage is thought to result from prostaglandin-mediated hyperfiltration injury and repeated microinfarction, which causes interstitial scarring and remodeling of the renal vasculature and prohibits proper countercurrent exchange mechanisms (8,20,27). Secondarily, back pressure transmitted to submucosal blood vessels causes hemorrhage into the renal pelvis and subsequent hematuria (8); of note, we found no obvious radiologic evidence of

iron in the renal pelvis. In many tissues, cellular iron buildup can trigger a redox cascade beginning with lipid peroxidation and lysosomal instability, activation of the apoptotic caspase system, direct protein and DNA denaturation, and release of inflammatory mediators (2,11,14). In an experimental rat model, Zhou et al (14) found that iron overloading of specimens led to kidney iron deposition, proteinuria, tubular atrophy, and interstitial fibrosis—a picture similar to the clinical features of SCD nephropathy. Chronic renal failure, tubular dysfunction, and hypertension (the same clinical phenotype as SCD) has also been described in paroxysmal nocturnal hemoglobinuria (41). Our study, because of its retrospective nature, neither supports nor rejects a direct, toxic role for kidney iron. The only routinely accessible parameters of kidney function, including serum creatinine, blood pressure, and kidney volumes, are too crude to draw any conclusions. Furthermore the patients were young and received chronic transfusions; both of which tended to lessen the prevalence of detectable kidney disease. Future work should include more sensitive markers of proximal tubule function such as *n*-acetyl-β-glucosaminidase (NAG) and β_2-microglobulin (38). Studies should also be broadened to examine nontransfused patients with SCD.

Our study suffered from the following technical limitations. We did not strictly divide ROIs in the kidney into cortex and medulla because partial volume effects made this distinction subjective. While our approach provided an accurate assessment of average kidney iron, it grossly underestimates cortical iron concentrations. It is possible that proper segmentation might improve pathophysiologic correlation and this should be investigated in future studies. Additionally, while our choice of echo spacing is well suited for quantifying high levels of tissue iron, it is far less sensitive at detecting slight increases in tissue iron. A technique that uses longer echo time spacing, such as blood oxygen level-dependent (BOLD) MRI, would have been useful to detect a more delicate elevation in tissue iron in TM kidneys compared to normal. It is possible that TM patients have more subtle cortical or medullary changes in R2* that our techniques were not optimized to observe. BOLD MRI has been used in human and animal studies to assess kidney oxygenation, and yield R2* estimates similar to those observed in our normal population (42,43). It is unclear whether BOLD techniques retain their sensitivity in the presence of iron overload but could potentially be used to monitor vascular changes in TM and SCD kidneys as well. Lastly, our constant-plus-monoexponential model is ideally suited for unsupervised pixelwise mapping of heavy iron concentrations, but slightly overestimates R2* at lower iron concentrations and would be less well suited for BOLD studies (44).

In summary, we confirmed that cortical kidney iron deposition is common in SCD and not TM. Kidney iron results from chronic hemolysis and is uncorrelated to total body iron overload. Kidney iron decreases over time in chronically transfused SCD patients representing iron elimination through chelation therapy and somatic growth. Prospective studies are needed to determine if kidney iron deposition impairs renal tubular function and whether it effectively predicts the onset or severity of SCD systemic and pulmonary vasculopathy.

REFERENCES

1. Angastiniotis M, Modell B. Global epidemiology of hemoglobin disorders. Ann N Y Acad Sci 1998;850:251–269.
2. Gordeuk VR, Bacon BR, Brittenham GM. Iron overload: causes and consequences. Annu Rev Nutr 1987;7:485–508.
3. Brittenham GM, Badman DG. Noninvasive measurement of iron: report of an NIDDK workshop. Blood 2003;101:15–19.
4. Wood JC, Enriquez C, Ghugre N, et al. MRI R2 and R2* mapping accurately estimates hepatic iron concentration in transfusion-dependent thalassemia and sickle cell disease patients. Blood 2005;106:1460–1465.
5. Ghugre NR, Enriquez CM, Gonzalez I, Nelson MD Jr, Coates TD, Wood JC. MRI detects myocardial iron in the human heart. Magn Reson Med 2006;56:681–686.
6. Ghugre N, Enriquez C, Wood JC. Myocardial R2 and R2* vary linearly with cardiac iron in human heart. In: Proc 13th Annual Meeting ISMRM, Miami Beach, FL; 2005.
7. Wood JC, Otto-Duessel M, Aguilar M, et al. Cardiac iron determines cardiac T2*, T2, and T1 in the gerbil model of iron cardiomyopathy. Circulation 2005;112:535–543.
8. Buckalew VM Jr, Someren A. Renal manifestations of sickle cell disease. Arch Intern Med 1974;133:660–669.
9. Lande IM, Glazer GM, Sarnaik S, Aisen A, Rucknagel D, Martel W. Sickle-cell nephropathy: MR imaging. Radiology 1986;158:379–383.
10. Solecki R, von Zglinicki T, Muller HM, Clausing P. Iron overload of spleen, liver and kidney as a consequence of hemolytic anaemia. Exp Pathol 1983;23:227–235.
11. Tracz MJ, Alam J, Nath KA. Physiology and pathophysiology of heme: implications for kidney disease. J Am Soc Nephrol 2007;18:414–420.
12. Gburek J, Verroust PJ, Willnow TE, et al. Megalin and cubilin are endocytic receptors involved in renal clearance of hemoglobin. J Am Soc Nephrol 2002;13:423–430.
13. Jeong JY, Kim SH, Lee HJ, Sim JS. Atypical low-signal-intensity renal parenchyma: causes and patterns. Radiographics 2002;22:833–846.
14. Zhou XJ, Laszik Z, Wang XQ, Silva FG, Vaziri ND. Association of renal injury with increased oxygen free radical activity and altered nitric oxide metabolism in chronic experimental hemosiderosis. Lab Invest 2000;80:1905–1914.
15. Bayazit AK, Noyan A, Aldudak B, et al. Renal function in children with sickle cell anemia. Clin Nephrol 2002;57:127–130.
16. Buhl L, Muirhead DE, Prentis PF. Renal hemosiderosis due to thalassemia: a light and electron microscopy study with electron probe X-ray microanalysis. Ultrastruct Pathol 1993;17:169–183.
17. Koliakos G, Papachristou F, Koussi A, et al. Urine biochemical markers of early renal dysfunction are associated with iron overload in beta-thalassaemia. Clin Lab Haematol 2003;25:105–109.
18. Michelakakis H, Dimitriou E, Georgakis H, et al. Iron overload and urinary lysosomal enzyme levels in beta-thalassaemia major. Eur J Pediatr 1997;156:602–604.
19. Ong-ajyooth L, Malasit P, Ong-ajyooth S, et al. Renal function in adult beta-thalassemia/Hb E disease. Nephron 1998;78:156–161.
20. Saborio P, Scheinman JI. Sickle cell nephropathy. J Am Soc Nephrol 1999;10:187–192.
21. Ghugre NR, Enriquez CM, Coates TD, Nelson MD Jr, Wood JC. Improved R2* measurements in myocardial iron overload. J Magn Reson Imaging 2006;23:9–16.
22. Dinkel E, Ertel M, Dittrich M, Peters H, Berres M, Schulte-Wissermann H. Kidney size in childhood. Sonographical growth charts for kidney length and volume. Pediatr Radiol 1985;15:38–43.
23. Olivieri NF, Brittenham GM. Iron-chelating therapy and the treatment of thalassemia. Blood 1997;89:739–761.
24. Angelucci E, Brittenham GM, McLaren CE, et al. Hepatic iron concentration and total body iron stores in thalassemia major. N Engl J Med 2000;343:327–331.
25. Kato GJ, McGowan V, Machado RF, et al. Lactate dehydrogenase as a biomarker of hemolysis-associated nitric oxide resistance, priapism, leg ulceration, pulmonary hypertension, and death in patients with sickle cell disease. Blood 2006;107:2279–2285.

26. Morris CR, Kato GJ, Poljakovic M, et al. Dysregulated arginine metabolism, hemolysis-associated pulmonary hypertension, and mortality in sickle cell disease. JAMA 2005;294:81–90.
27. Nasr SH, Markowitz GS, Sentman RL, D'Agati VD. Sickle cell disease, nephrotic syndrome, and renal failure. Kidney Int 2006;69: 1276–1280.
28. Lee JW, Kim SH, Yoon CJ. Hemosiderin deposition on the renal cortex by mechanical hemolysis due to malfunctioning prosthetic cardiac valve: report of MR findings in two cases. J Comput Assist Tomogr 1999;23:445–447.
29. Suzukawa K, Ninomiya H, Mitsuhashi S, Anno I, Nagasawa T, Abe T. Demonstration of the deposition of hemosiderin in the kidneys of patients with paroxysmal nocturnal hemoglobinuria by magnetic resonance imaging. Intern Med 1993;32:686–690.
30. Kumpers P, Herrmann A, Lotz J, Mengel M, Schwarz A. A blue kidney—chronic renal failure as a consequence of siderosis in paroxysmal nocturnal hemoglobinuria? Clin Nephrol 2006;66:210–213.
31. Mathieu D, Rahmouni A, Villeneuve P, Anglade MC, Rochant H, Vasile N. Impact of magnetic resonance imaging on the diagnosis of abdominal complications of paroxysmal nocturnal hemoglobinuria. Blood 1995;85:3283–3288.
32. Roubidoux MA. MR of the kidneys, liver, and spleen in paroxysmal nocturnal hemoglobinuria. Abdom Imaging 1994;19:168–173.
33. Siegelman ES, Mitchell DG, Semelka RC. Abdominal iron deposition: metabolism, MR findings, and clinical importance. Radiology 1996;199:13–22.
34. Siegelman ES, Outwater E, Hanau CA, et al. Abdominal iron distribution in sickle cell disease: MR findings in transfusion and nontransfusion dependent patients. J Comput Assist Tomogr 1994;18:63–67.
35. Lezcano NE, Odo N, Kutlar A, Brambilla D, Adams RJ. Regular transfusion lowers plasma free hemoglobin in children with sickle-cell disease at risk for stroke. Stroke 2006;37:1424–1426.
36. Chalevelakis G, Clegg JB, Weatherall DJ. Imbalanced globin chain synthesis in heterozygous beta-thalassemic bone marrow. Proc Natl Acad Sci U S A 1975;72:3853–3857.
37. Aldudak B, Karabay Bayazit A, Noyan A, et al. Renal function in pediatric patients with beta-thalassemia major. Pediatr Nephrol 2000;15:109–112.
38. Voskaridou E, Terpos E, Michail S, et al. Early markers of renal dysfunction in patients with sickle cell/beta-thalassemia. Kidney Int 2006;69:2037–2042.
39. Gladwin MT, Sachdev V, Jison ML, et al. Pulmonary hypertension as a risk factor for death in patients with sickle cell disease. N Engl J Med 2004;350:886–895.
40. Powars DR, Chan LS, Hiti A, Ramicone E, Johnson C. Outcome of sickle cell anemia: a 4-decade observational study of 1056 patients. Medicine (Baltimore) 2005;84:363–376.
41. Clark DA, Butler SA, Braren V, Hartmann RC, Jenkins DE Jr. The kidneys in paroxysmal nocturnal hemoglobinuria. Blood 1981;57: 83–89.
42. Sadowski EA, Fain SB, Alford SK, et al. Assessment of acute renal transplant rejection with blood oxygen level-dependent MR imaging: initial experience. Radiology 2005;236:911–919.
43. Prasad PV, Edelman RR, Epstein FH. Noninvasive evaluation of intrarenal oxygenation with BOLD MRI. Circulation 1996;94:3271–3275.
44. Ghugre N, Enriquez C, Coates TD, Nelson MD, Wood JC. Improved R2* measurements in myocardial iron overload. J Cardiovasc Magn Reson 2005;7:32–33.